Materials Science in Semiconductor Processing 82 (2018) 112–125

Contents lists available at ScienceDirect

Materials Science in Semiconductor Processing

journal homepage: www.elsevier.com/locate/mssp

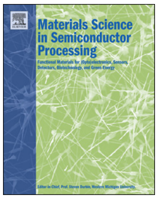

Material removal of single crystal 4H-SiC wafers in hybrid laser-waterjet micromachining process

Shaochuan Feng[a,b], Chuanzhen Huang[a,*], Jun Wang[b,*], Hongtao Zhu[a]

[a] *Center for Advanced Jet Engineering Technologies (CaJET), Key Laboratory of High-Efficiency and Clean Mechanical Manufacture (Ministry of Education), School of Mechanical Engineering, Shandong University, Jinan 250061, China*
[b] *School of Mechanical and Manufacturing Engineering, The University of New South Wales (UNSW), Sydney, NSW 2052, Australia*

ARTICLE INFO

Keywords:
Hybrid micromachining
Laser
Waterjet
Material removal
Finite difference method (FDM)

ABSTRACT

Yield stress, as well as ultimate stress, decreases with an increased temperature. A much smaller cutting force can be applied to perform the machining at high temperatures. Material is considered “softened” when its yield and ultimate stresses decrease due to the increase of temperature. During the hybrid laser-waterjet micromachining process, the material is heated by laser. Once the critical resolved shear stress (CRSS), related to the yield stress, decreases to be equal to the applied resolved shear stress induced by the pressurized waterjet impingement, the material begins to be deformed and then removed plastically. The hybrid laser-waterjet micromachining technology shows a satisfying performance on almost damage-free and high-efficient micromachining of thermal-sensitive and hard-brittle materials at their “softened” status. The present study is focused on the material removal mechanism of single crystal 4H-SiC in the hybrid laser-waterjet micromachining process. The temperature-dependent CRSS on the primary slip system of 4H-SiC is formulated. It is shown that the CRSS of 4H-SiC is less than 5 MPa at 1650 K. The shear stress induced by pressurized waterjet impingement, laser heating effect under the laser-water interference and the waterjet cooling effect are respectively studied. The range of water pressure used in the machining process is from 4 MPa to 13 MPa. A 2-D numerical model is developed using the finite difference method (FDM). The simulations show that the material begins to be removed before the laser intensity reaches its maximum in a laser pulse cycle. The depth and width of the microgroove increase gradually in the following several cycles. The increments become gradually less until this increase stops. The material is removed before it’s heated to its melting temperature and at a softened but still solid status. Heat accumulation between laser pulses is not expected in the process. The machined surface quality and material removal mechanisms of the hybrid laser-waterjet micromachining and laser dry ablation are compared by 3D profiles and SEM photographs of the microgrooves obtained from these two machining methods. The surface quality obtained from hybrid laser-waterjet micromachining is better than that obtained from laser dry ablation. The protrusion strips along the cut edges of laser dry ablation are scaly and similar to welded junction. It indicates that the material is melted or vaporized by laser heating and re-solidified at cut edges to form a recast layer during laser dry ablation. There aren’t recast layers on the machined surface of hybrid laser-waterjet micromachining. Its surface texture is characterized as a typical feature of plastic slip.

1. Introduction

Laser ablation removes material efficiently without cutting force and pollution. However, laser ablation process is usually accompanied by thermal damages. As compared to conventional nanosecond laser dry ablation, ultra-short pulsed laser (e.g. femtosecond laser) reduces thermal damages but with much lower machining efficiency [1]. Applying water in nanosecond laser ablation is an effective approach to reduce thermal damages. Waterjet guided laser ablation technology is based on guiding a laser beam inside a fine waterjet [2]. The fine waterjet is used as “liquid fiber with variable length”. The coupling of laser and waterjet is with some difficulty. Besides, there are some other water assisted laser ablation technologies such as underwater laser ablation [3,4] and waterjet assisted laser ablation [5]. In water assisted laser ablation processes, materials are removed due to melting, evaporation and thermal shock.

For most ceramics and semiconductor materials, their high-temperature yield stresses (as well as ultimate stresses) and hardness are much lower than that at room temperature. Therefore, a much smaller cutting force can be applied to perform the machining at high

---

* Corresponding authors.
E-mail addresses: fengshaochuan@mail.sdu.edu.cn (S. Feng), chuanzhenh@sdu.edu.cn (C. Huang), jun.wang@unsw.edu.au (J. Wang), htzhu@sdu.edu.cn (H. Zhu).

https://doi.org/10.1016/j.mssp.2018.03.035
Received 27 November 2017; Received in revised form 7 March 2018; Accepted 28 March 2018
1369-8001/ © 2018 Elsevier Ltd. All rights reserved.

Nomenclature

A_s	cross-sectional area of microgroove (m^2)
a_b	optical absorption coefficient of material (1/m)
b	length scale related to wall pressure (m)
c_w	specific heat capacity of water ($J\,kg^{-1}\,K^{-1}$)
D	laser beam diameter before focused by lens (m)
d_b	laser spot diameter (m)
d_{fR}	focused laser diameter after refraction (m)
d_s	distance from stagnation point (m)
d_w	nozzle orifice diameter (m)
F	focal length of lens (m)
f	laser pulse frequency (Hz)
$g_0(\eta)$, $g_*(\eta)$	functions of η
h	convection heat transfer coefficient ($W\,m^{-2}\,K^{-1}$)
h_c	thermal contact conductance coefficient ($W\,m^{-2}\,K^{-1}$)
h_1	average convection heat transfer coefficient for impingement region ($W\,m^{-2}\,K^{-1}$)
h_2	average convection heat transfer coefficient for wall jet region ($W\,m^{-2}\,K^{-1}$)
k	thermal conductivity of material ($W\,m^{-1}\,K^{-1}$)
k_w	thermal conductivity of water ($W\,m^{-1}\,K^{-1}$)
L_f	laser focus height (without considering refraction) (m)
L_{fR}	laser focus height after refraction (m)
L_s	nozzle stand-off distance (m)
L_1	characteristic length of impingement region (m)
L_2	characteristic length of wall jet region (m)
l_a	light absorption length in water (m)
l_w	water layer thickness (m)
M_R^2	laser beam quality factor in water
n_w	refractive index of water
P_l	average laser power (W)
P_w	inlet water pressure (Pa)
Q	laser heat source (W/m^3)
q_m	coefficient
R_f	material reflectivity
R_w	water reflectivity
s	eccentricity of stagnation point (m)
T	temperature (K)
T_b	break temperature (K)
T_f	surrounding temperature (K)
t	time (s)
v	traverse speed of hybrid cutting head (m/s)
v_R	material removal rate (m^3/s)
v_0	initial waterjet velocity (m/s)
x_w	waterjet offset distance (m)
x, y	space coordinates parallel to material surface (m)
z	space coordinate normal to material surface (m)
α	thermal diffusivity of material (m^2/s)
γ	angle between wall shear stress direction and slip direction (°)
γ_d	one-side beam divergence angle (°)
η	dimensionless scale
θ	waterjet inclination angle (°)
ι	laser pulse overlap
λ	laser wavelength (m)
μ	dynamic viscosity of water (Pa s)
ρ_w	water density (kg/m^3)
σ_m	coefficient
τ	wall shear stress (Pa)
τ_c	critical resolved shear stress (Pa)
τ_m	maximum wall shear stress (Pa)
τ_p	laser pulse duration (s)
τ_R	applied resolved shear stress (Pa)
φ	laser pulse shape function in time domain
ψ	laser pulse shape function in space domain
O	intersection of jet centerline and material surface
S	stagnation point

temperatures. Material is considered “softened” when its yield stress and hardness decrease due to the increase of temperature.

When the temperature is higher than the material brittle-to-ductile transition (BDT) temperature, the machining is performed under the ductile regime [6]. Virkar et al. [7] and Patten et al. [8] numerically and experimentally investigated the effects of laser heating on the material removal process where single crystal 4H-SiC was machined using ductile mode micro-laser assisted machining. They proposed that the cutting force is reduced when machining is conducted above the thermally softening temperature.

Tangwarodomnukun et al. [9] combined the advantages of laser processing with those of waterjet cutting and proposed a hybrid laser-waterjet micromachining technology. Waterjet is applied off-axially to expel the material heated softened by laser radiation and cool the material to eliminate thermal damages during the material removal process. In the hybrid laser-waterjet micromachining process, the critical resolved shear stress (CRSS), related to the yield stress, decreases due to laser heating. Once the CRSS decreases to be equal to the applied resolved shear stress induced by the pressurized waterjet impingement, the material begins to be deformed and then removed plastically. Consequently, the material can be removed below its melting temperature at a softened but still solid status.

In our earlier study [10], it has been shown on micromachining single crystal silicon carbide (SiC) that this hybrid laser-waterjet micromachining technology can remove material nearly ideally and conduct almost damage-free micromachining of materials. This machining technology can be used to replace etching (non-through cuts) as well as slicing and dicing (through cuts) of semiconductors without process induced damages. Besides, Wang et al. [11] experimentally investigated hybrid laser-waterjet micro-milling where machining is performed in a multi-pass approach.

There is complex interaction of laser, waterjet and material under the coupled effect of laser heating and waterjet expelling as well as cooling during the hybrid laser-waterjet micromachining process. Moreover, it has been found that the process characteristics of this technology are highly dependent on the target material being processed. The present study is focused on the material removal mechanism of single crystal 4H-SiC in the hybrid laser-waterjet micromachining process.

In the most common polytypes of SiC, 4H, 6H, 15R and 3C, the letters H, R and C denote a hexagonal, rhombohedral and cubic structure, respectively, and the number before the letters denotes the periodicity of tetrahedrons along the [0001] (or [111] in the case of cubic) *c*-axis of the crystal [12]. For hexagonal close-packed (HCP) crystals, the slip systems depend on the *c*/*a* ratio of the crystal unit cell. As this ratio of 4H-SiC is 3.273 [13], which is greater than 1.633, its only slip system is (0001) $<11\bar{2}0>$, namely the primary slip system. Correspondingly, the slip occurring on the primary slip system is named as a basal slip. Samant et al. [12] conducted the studies on the basal slip of 4H-SiC at high temperatures. The relationship between the temperature and the CRSS was experimentally studied under strain rates of $3.1 \times 10^{-5}\,s^{-1}$, $6.3 \times 10^{-5}\,s^{-1}$, $1.3 \times 10^{-4}\,s^{-1}$ and $6.5 \times 10^{-4}\,s^{-1}$. Meanwhile, Demenet et al. [14] investigated this relationship under strain rates of $2.6 \times 10^{-6}\,s^{-1}$ and $3.6 \times 10^{-5}\,s^{-1}$. There is also a study under a strain rate of $3.0 \times 10^{-5}\,s^{-1}$ that was conducted by Mussi et al. [15]. Their results show that with the increasing of temperature, the CRSS decreases significantly. This trend is independent of strain rate.

It seems that considering the shear stress induced by pressurized

Download English Version:

https://daneshyari.com/en/article/7117650

Download Persian Version:

https://daneshyari.com/article/7117650

Daneshyari.com